Conf-9309352--1

DOE/ER/40427-31-N93

A QUARK MODEL OF $\bar{\Lambda}\Lambda$ PRODUCTION OF $\bar{p}p$ INTERACTIONS

M.A. Alberg[(1),(2)], E.M. Henley[(2)], L. Wilets[(2)], and P.D. Kunz[(3)]

[(1)] *Department of Physics, Seattle University, Seattle, Washington 98122 USA*
[(2)] *Department of Physics, FM-15, University of Washington, Seattle, WA 98195, USA*
[(3)] *Nuclear Physics Laboratory, University of Colorado, Boulder, Colorado 80309 USA*

To be published in "Journal of Atomic Nuclei"
Paper given at "2nd Biennial Workshop on Nuclear - Antinuclear Physics"
ITEP, Moscow, Russia, 13th - 18th Sept. 1993.

A QUARK MODEL OF $\bar{\Lambda}\Lambda$ PRODUCTION IN $\bar{p}p$ INTERACTIONS

M.A. Alberg[(1),(2)], E.M. Henley[(2)], L. Wilets[(2)] and P.D. Kunz[(3)]

[(1)] *Department of Physics, Seattle University, Seattle, Washington 98122 USA*

[(2)] *Department of Physics, University of Washington, Seattle, Washington 98195 USA*

[(3)] *Nuclear Physics Laboratory, University of Colorado, Boulder, Colorado 80309 USA*

ABSTRACT

A quark model which includes both scalar and vector contributions to the reaction mechanism (SV quark model) is used in a DWBA calculation of $\bar{\Lambda}\Lambda$ production in $\bar{p}p$ interactions. Total and differential cross-sections, polarizations, depolarizations, and spin-correlation coefficients are computed for laboratory momenta from threshold to 1695 MeV/c. The free parameters of the calculation are the scalar and vector strengths, a quark cluster size parameter, and the parameters of the unknown $\bar{\Lambda}\Lambda$ potentials. Good agreement with experiment is found for constructive interference of the scalar and vector terms, and for $\bar{\Lambda}\Lambda$ potentials which differ from those suggested by several authors on the basis of SU(3) arguments. The fit to the data is better than that obtained by other quark models, which use only scalar *or* vector annihilation terms. The agreement with experiment is also better than that found in meson-exchange models. The recent suggestion [1] that measurement of the depolarization parameter D_{nn} can be used to discriminate between meson-exchange and quark models is examined in detail. We conclude that a measurement of D_{nn} will provide a test of which of these models, as presently constructed, is the more appropriate description of strangeness production in the $\bar{p}p \rightarrow \bar{\Lambda}\Lambda$ reaction.

Speaker: M.A. Alberg, Department of Physics, Seattle University, Seattle WA 98122, USA.. E-mail: alberg@uwaphast.bitnet. FAX: (206) 685-0635.

1. Introduction

We describe the results of a DWBA calculation of the total and differential cross sections, polarizations, and spin-correlation coefficients that have been measured by the PS185 collaboration [2] for the reaction $\bar{p}p \rightarrow \bar{\Lambda}\Lambda$ from threshold to 1695 MeV/c. We also present predictions for the proposed measurement [3] of the depolarization parameter D_{nn}. The $pp \rightarrow \bar{\Lambda}\Lambda$ reaction can be described in terms of either quark or meson-exchange models, and may provide a test of which picture is more appropriate at the momenta and distances which correspond to the experimental measurements. Because the reaction is very sensitive to initial and final state interactions it also can provide information about the $\bar{\Lambda}\Lambda$ interaction, for which there are no direct experimental measurements.

Several groups have used meson-exchange models [4-9] to obtain reasonable fits to the data. The K, K^* and K^{**} exchanges in these models are of short range, at distances for which one might expect quark degrees of freedom to be important. Quark models provide a microscopic picture of the reaction which tests our understanding of non-perturbative QCD. In the simplest quark models either a scalar ("$^3P_0$") or vector ("$^3S_1$") interaction is assumed to describe $\bar{q}q$ annihilation and creation, and several calculations [6,10-15] have obtained reasonable agreement with experiment. In some cases these results have been used to argue that either the scalar or vector interaction provides the correct description of annihilation. We have proposed [16] that both mechanisms should be included, since by analogy with the NN interaction one would expect at least vector exchange (of one or more gluons) and a scalar representation of both confinement and multigluon exchange.

In theoretical calculations to date, quark and meson-exchange models have been about equally successful in fitting experimental data, although our SV quark model is better at reproducing the steep rise seen in the differential cross-section at forward angles. Recently the Jülich group has proposed [1] that the depolarization parameter D_{nn} could be used to discriminate between the quark and meson-exchange models. The quark model they used was the vector mechanism proposed by Kohno and Weise [6]. We have carried out calculations of D_{nn} for our SV model, and find that even with the inclusion of the scalar term in the reaction mechanism, the quark model predictions differ strongly from those of meson-exchange.

Sections 2 through 5 provide a summary of our quark model calculation, including comparison with experimental results and with other quark and meson-exchange models. A complete description of the calculation, together with comparisons to experimental data of PS185 for the $\bar{p}p \to \bar{\Lambda}\Lambda$ reaction, has recently been published [17]. In section 6 we compare our SV quark model predictions for D_{nn} to the meson-exchange calculations of the Jülich group.

2. Reaction Mechanism

Our reaction mechanism includes both scalar and vector contributions to the annihilation and creation of antiquark-quark pairs. The simplest graphs for these terms are shown in Fig. 1. The "$^3P_0$" term represents scalar multigluon exchange and/or the confining scalar force, whereas the "$^3S_1$" term represents vector exchange of one or more gluons. Both terms also include $\bar{q}q$ pairs in intermediate states. In our model, the operator for scalar exchange is zero-range and of the form

$$I_s = g_s \boldsymbol{\sigma}'_3 \cdot \left(\frac{\boldsymbol{\nabla}_{3'} - \boldsymbol{\nabla}_{6'}}{2m_s} \right) \boldsymbol{\sigma}_3 \cdot \left(\frac{\boldsymbol{\nabla}_3 - \boldsymbol{\nabla}_6}{2m} \right) , \tag{1}$$

and that for vector exchange is

$$I_v = g_v \boldsymbol{\sigma}'_3 \cdot \boldsymbol{\sigma}_3 \tag{2}$$

In (1), m_s is the strange quark mass and m is the up quark mass. For $\bar{\Lambda}\Lambda$ production the active quarks are a $\bar{u}u$ pair which is annihilated and an $\bar{s}s$ pair which is created.

The spectator quark pairs, $\bar{u}\bar{d}$ and ud, must each be in an I=0 and S=0 state, so that the spin of the $\bar{\Lambda}\Lambda$ pair is carried by the strange quarks. Both scalar and vector terms are spin triplet, so our quark model predicts a singlet fraction for the $\bar{\Lambda}\Lambda$ pair which is identically zero, in good agreement with experiment. A singlet contribution can arise, e.g. from a pseudoscalar "$^1S_0$" term, but this has been shown to be small [18].

3. Initial and Final State Interactions

3.1. THE $\bar{p}p$ INTERACTION

In most of our work we use the $\bar{p}p$ potential proposed by Kohno and Weise [6]

$$V_{\bar{N}N}(r) = U_{\bar{N}N}(r) + iW_{\bar{N}N}(r) \tag{3}$$

in which the real term $U_{\bar{N}N}(r)$ includes central, tensor, spin-orbit and spin-spin terms and the imaginary term $W_{\bar{N}N}(r)$ is a central potential which represents annihilation. The long-range part of $U_{\bar{N}N}(r)$ is determined by the G-parity transform of Ueda's [19] one-boson exchange potential. For r < 1 fm each term in the real part of the potential is extrapolated smoothly to the origin by means of a Woods-Saxon form. The imaginary potential $W_{\bar{N}N}(r)$ is given by:

$$W_{\bar{N}N}(r) = W^{(0)}_{\bar{N}N}\left\{1 + \exp[(r - r_0)/a]\right\}^{-1} \tag{4}$$

with r_0 = 0.55 fm, a = 0.2 fm, and $W^{(0)}_{\bar{N}N} = -1.2$ GeV. These parameters give good fits to total, elastic, annihilation and charge-exchange $\bar{p}p$ data for lab momenta up to 2.5 GeV/c.

3.2. THE $\bar{\Lambda}\Lambda$ INTERACTION

Our $\bar{\Lambda}\Lambda$ potential is chosen to be of the form used by Kohno and Weise [6], although we find it necessary to vary the parameters of that potential to get good agreement with experiment. In the Kohno-Weise $\bar{\Lambda}\Lambda$ potential

$$V_{\bar{\Lambda}\Lambda}(r) = U_{\bar{\Lambda}\Lambda}(r) + iW_{\bar{\Lambda}\Lambda}(r) \tag{5}$$

the real term $U_{\bar{\Lambda}\Lambda}(r)$ represents isoscalar meson exchange and the imaginary term $W_{\bar{\Lambda}\Lambda}(r)$ represents annihilation. The long-range part of $U_{\bar{\Lambda}\Lambda}(r)$ is derived from the isoscalar exchanges of the Nijmegen YN potential [20], in which SU(3) relations were used to determine couplings for the pseudoscalar, vector, and scalar nonets. As in the $\bar{N}N$ case, the short-range part is determined by means of a smooth extrapolation to the origin. The imaginary term $W_{\bar{\Lambda}\Lambda}(r)$ is taken to be a Woods-Saxon form with the same radius and diffuseness as the $\bar{N}N$ absorptive potential:

$$W_{\bar{\Lambda}\Lambda}(r) = W^{(0)}_{\bar{\Lambda}\Lambda}\left\{1 + \exp[(r - r_0)/a]\right\}^{-1} \tag{6}$$

The strength $W^{(0)}_{\bar{\Lambda}\Lambda}$ = -700 MeV was chosen to fit the $\bar{\Lambda}\Lambda$ production cross-section. The Kohno-Weise potential described above is based in part on SU(3) symmetry arguments together with the use of the G-parity transformation, both of which may be questioned. In the absence of direct experimental data on the $\bar{\Lambda}\Lambda$ interaction, this potential is a good starting point for our analysis. But as we describe in the next section, good fits to the experimental data require changes in the parameters of the potential, and thereby give us information about the $\bar{\Lambda}\Lambda$ interaction that has not been previously available.

4. Comparison with Experiment

A nine-parameter fit was made to the PS185 data reported at lab momenta of 1436, 1437, 1445, 1477, 1508, 1546, 1642 and 1695 MeV/c. The 356 data points included in this set of measurements include differential cross sections, polarizations and spin correlation coefficients. No data points were excluded from the fits.

Minimization programs which included Monte Carlo, simplex, gradient, and simulated annealing techniques were used to search for the best values of g_v (the strength of the vector term), g_s (the strength of the scalar term), r_0 (a range parameter in the quark Gaussian wave function), and six parameters in the $\bar{\Lambda}\Lambda$ potential. The searches were started with the Kohno-Weise values for the $\bar{\Lambda}\Lambda$ potential parameters. Three parameters for the real part of the potential were varied: V (the strength of the central plus spin-spin term), V_T (the strength of the tensor term), and V_{LS} (the strength of the spin-orbit term). Three parameters were varied in the annihilation term: $W^{(0)}_{\bar{\Lambda}\Lambda}$, r_w and a_w (the strength, radius and diffuseness of the potential). We considered three possible cases for the reaction mechanism: the vector "$^3S_1$" term alone, the scalar "$^3P_0$" term alone, and a superposition of both terms. The results of our searches are shown in Table 1. All of our searches found minima for very small values of a_w, the diffuseness of the annihilation potential. We therefore fixed a_w at the value of 0.01 fm to avoid reflections from a sharp square-well potential, which left 8 free parameters to be varied in our searches. Clearly the superposition of both terms provides the best fit to the data, with a χ^2 per data point of 3.2. An example of the quality of our fit to the data using our best global fit parameters is shown in Fig. 2. A complete comparison with all experimental data is given in reference 17. The best global fit parameters given in Table 1 indicate that the $\bar{\Lambda}\Lambda$ potential differs from that expected on the basis of SU(3) arguments. In the real part of the potential, for which the long-range behavior is determined by one-boson exchange, the central term is small. The tensor and spin-orbit terms are much larger than the predictions of the one-boson exchange model. This may reflect a greater spin-dependence in the interaction, which has also been noted by other investigators [7-9]. The annihilation term in the $\bar{\Lambda}\Lambda$ potential is deeper, longer in range, and much less diffuse than the Kohno-Weise annihilation potential.

In Fig. 3 we show a comparison of the best vector alone, scalar alone, and combined reaction mechanism calculations with the experimental data at 1642 MeV/c. Here it is seen that both terms are needed in the reaction mechanism to get a good fit to both the differential cross section and polarization data. These results are representative of all the laboratory momenta studied. Vector or scalar terms alone can fit the differential cross sections reasonably well, but only a superposition fits the spin observables as well.

5. Comparison to other Theoretical Calculations

5.1 QUARK MODELS

Quark model calculations of differential cross sections and polarizations have been made by Kohno and Weise [6] and Furui and Faessler [14]. Kohno and Weise used the vector "$^3S_1$" model with the initial and final state interactions we have described above. Furui and Faessler considered separately the vector "$^3S_1$" and the scalar "$^3P_0$" models, with initial and final state interactions taken from the meson-exchange calculations of Tabakin and Eisenstein [4]. They concluded that their "$^3P_0$" model was in better agreement with the data. The results of both calculations are compared to ours and to the data in Fig. 4. Our calculations are in better agreement with the differential cross sections. The Fur . and Faessler calculations and ours have approximately equally good fits to the polari. ation, but they predict a second "zero-crossing" in the backward direction, which is not seen in the data. Thus, both scalar and vector reaction mechanisms are needed for a good fit to the data, as we have argued above.

5.2 MESON-EXCHANGE MODELS

Meson-exchange models have been proposed by Tabakin and Eisenstein [4], Niskanen [5], Kohno and Weise [6], Timmermans et al. [7], LaFrance et al. [8] and Haidenbauer et al. [9]. These models differ in the types of K-mesons included in the exchange (K, K*, K**) and in their initial and final state interactions. The earlier calculations [4,5] had a limited amount of experimental data with which to compare their results. Kohno and Weise's meson-exchange results were similar to their quark model calculations, which we have discussed above. A comparison of our results with the later meson-exchange calculations is given in Fig. 5 for laboratory momenta of 1508 MeV/c and 1695 MeV/c. Our fits are better than those of LaFrance et al. and Haidenbauer et al., each of which fails to reproduce the steep forward rise in the differential cross section at 1695 MeV/c and predicts oscillatory behavior in the polarization at that momentum which is not seen in the experiment. Our fit to the differential cross section and polarization is as good as that of the Nijmegen group [7].

6. Depolarization

Haidenbauer et al. [1] have proposed that a measurement of the depolarization parameter D_{nn} could be used to discriminate between quark and meson-exchange models. This spin observable measures the depolarization of the target in a direction $\hat{n}$ normal to the reaction plane [21]

$$D_{nn} = \frac{tr\,(\sigma_n^{\Lambda}\, M\, \sigma_n^{p} M^{\dagger})}{tr\,(M M^{\dagger})} \tag{7}$$

in which M is the reaction matrix element.

Haidenbauer et al. noted that in Born approximation, the "tensor-type" interaction $\boldsymbol{\sigma}_1 \cdot \hat{\mathbf{r}}\, \boldsymbol{\sigma}_2 \cdot \hat{\mathbf{r}}$ which appears in meson exchange would predict $D_{nn} = -1$, whereas the vector quark interaction which includes the projection operator on the triplet state $P_1 = \frac{1}{4}(3 + \boldsymbol{\sigma}_1 \cdot \boldsymbol{\sigma}_2)$ would predict $D_{nn} = 2/3$. They found that a difference persisted even in the presence of initial and final state interactions, as shown in Fig. 6, taken from reference [1]. The meson-exchange calculations still predict $D_{nn} < 0$, and quark-model calculations predict $D_{nn} \gtrsim 0$. We have extended this comparison to our SV quark model, and find that the different predictions persist. In Fig. 7 we show calculations of D_{nn} at 3 different momenta. We have considered 4 sets of parameters. The first 3 are given in Table 1: our best global fit (both scalar and vector terms), our best global vector fit, and our best global scalar fit. In addition we considered the best combined vector and scalar fit at each momentum. In every case the depolarization calculated was

$\gtrsim 0$, and significantly different from the meson-exchange model results of Haidenbauer et al.

To test the sensitivity of our calculation to the choice of initial state interaction, we repeated the calculation using the Jülich "B" $\bar{p}p$ potential which corresponds to the solid curve of Fig. 6. Our $\bar{\Lambda}\Lambda$ parameters were varied to fit the experimental data at 1546 MeV/c. Again, as shown in Fig. 8, the depolarization remained $\gtrsim 0$. The difference between quark-model and meson-exchange model predictions for D_{nn} persists throughout the entire momentum range we have studied. The measurement of D_{nn} appears to be an excellent test of the models.

7. Conclusion

We have shown that an excellent fit to experimental data for the reaction $\bar{p}p \to \bar{\Lambda}\Lambda$ in the laboratory momentum region from 1436 to 1695 MeV/c can be obtained with a quark model that includes both scalar and vector terms in the reaction mechanism. This model is sensitive to both initial and final state interactions. In order to achieve good agreement with experiment, a $\bar{\Lambda}\Lambda$ potential which differs significantly from that expected on the basis of SU(3) arguments is required. The reaction takes place at distances for which quark effects are expected to be important, and our fits at lower momenta are comparable to the best of the meson-exchange calculations. At higher momenta our quark model better fits the steep rise in $d\sigma/d\Omega$ at forward angles. Further comparison at higher momenta and for the production of $\bar{\Sigma}\Lambda$, $\bar{\Lambda}\Sigma$ and $\bar{\Sigma}\Sigma$ pairs will help to distinguish between these models. The measurement of target depolarization D_{nn} appears to be a strong test of these complementary pictures of strangeness production in $\bar{p}p \to \bar{\Lambda}\Lambda$.

Acknowledgments

We wish to thank the members of the PS185 Collaboration for their interest in our calculations and the early communication of their results. We have enjoyed helpful conversations with R. Eisenstein, D. Hertzog, K. Holinde, K. Kilian, V. Mull, F. Tabakin, and W. Oelert. This work is supported in part by the U.S. Department of Energy. One of us (M.A.A.) was also supported in part by the National Science Foundation under Grant No. PHY-9223618.

References

1. J. Haidenbauer, K. Holinde, V. Mull and J. Speth, Phys. Lett. (1992) **B 291**, 223.
2. P.D. Barnes et al., Phys. Lett. (1987) **B189**, 249; Phys. Lett. (1989) **B229**, 432; Nucl. Phys. (1991) **A526**, 575; H. Fischer, Ph. D. Thesis, University of Freiburg, Germany (1992); W. Oelert (private communication).
3. H. Dutz et al., CERN/SPSLC 92-53, SPSLC/1192 (1992).
4. F. Tabakin and R.A. Eisenstein, Phys. Rev. (1985) **C31**, 1857.
5. J.A. Niskanen, Helsinki preprint HU-TFT-85-28.
6. M. Kohno and W. Weise, Phys. Lett. (1986) **B179**, 15; Phys. Lett. (1988) **B206**, 584; Nucl. Phys. (1988) **A479**, 433c.
7. R.G.E. Timmermans, T.A. Rijken and J.J. deSwart, Nucl. Phys. (1988) **A479**, 383c; Phys. Rev. (1992) **D45**, 2288.
8. P. LaFrance, B. Loiseau and R. Vinh Mau, Phys. Lett. (1988) **B214**, 317; Nucl. Phys. (1991) **A528**, 557.
9. J. Haidenbauer et al., Phys. Rev. (1992) **C45**, 931; J. Haidenbauer, K. Holinde, V. Mull and J. Speth, Phys. Rev. (1992) **C46**, 2158.
10. C.B. Dover and P.M. Fishbane, Nucl. Phys. (1984) **B244**, 349.
11. H. Genz and S. Tatur, Phys. Rev. (1984) **D30**, 63; G. Brix, H. Genz and S. Tatur, Phys. Rev. (1989) **D39**, 2054.

12. P. Kroll, B. Quadder and W. Schweiger, Nucl. Phys. (1989) **B316**, 373.

13. H.R. Rubinstein and H. Snellman, Phys. Lett. (1985) **B165**, 187.

14. S. Furui and A. Faessler, Nucl. Phys. (1987) **A468**, 669.

15. M. Burkardt and M. Dillig, Phys. Rev. (1988) **C37**, 1362.

16. M.A. Alberg, E.M. Henley and L. Wilets, Z. Phys. (1988) **331**, 207; M.A. Alberg, E.M. Henley, L. Wilets and P.D. Kunz, Nucl. Phys. (1990) **A508**, 323c.

17. M.A. Alberg, E.M. Henley, L. Wilets and P.D. Kunz, Nucl. Phys. (1993) **A560,** 365.

18. M.A. Alberg, E.M. Henley and W. Weise, Phys. Lett. (1991) **B255**, 498.

19. T. Ueda, Prog. Theor. Phys. (1979) **62**, 1670.

20. M.M. Nagels, T.A. Rijken and J.J. de Swart, Phys. Rev. (1975) **D12**, 744; Phys. Rev. (1977) **D15**, 2547; Phys. Rev. (1979) **D20**, 1633.

21. J. Bystricky, F. Lehar and P. Winternitz, J. Phys. (Paris) (1978) **39**, 1; P. LaFrance and P. Winternitz, J. Phys. (Paris) (1980) **41**, 1391.

Figure Captions

Fig. 1 Lowest order diagrams for $\bar{p}p \rightarrow \bar{\Lambda}\Lambda$.

Fig. 2 Differential cross section and polarization at 1642 MeV/c for our best global fit parameters. The experimental data is from PS185.

Fig. 3 A comparison of our best fits to the differential cross section and polarization data at 1642 MeV/c using the vector (dashed line), scalar (dot-dashed line) or combined vector and scalar (solid line) reaction mechanisms.

Fig. 4 Comparison of our calculations (solid line) with other quark-based models: the vector "$^3S_1$" model of Kohno and Weise [6] (dashed line) and the scalar "$^3P_0$" model of Furui and Faessler [14] (dot-dashed line).

Fig. 5 Comparison of our global best fit calculation (solid line) with the meson-exchange models of Timmermans et al.[7] (long-dashed line), LaFrance et al.[8] (short-dashed line), and Haidenbauer et al. [9] (dot-dashed line).

Fig. 6 Depolarization parameter D_{nn} as calculated by Haidenbauer et al. [1]. The solid and dashed lines correspond to meson-exchange calculations with different initial state interactions. The dot-dashed and dotted curves correspond to vector quark model calculations.

Fig. 7 Calculations of D_{nn} for 3 different momenta using the global fit parameters of Table 1: combined vector and scalar (solid line), vector (dashed line), scalar (dot-dashed line), and for the best combined vector and scalar fit parameters at each momentum (dotted line).

Fig. 8 Calculation of D_{nn} at 1546 MeV/c using the Jülich "B" $\bar{p}p$ potential for our combined vector and scalar (solid line), vector (dashed line) or scalar (dot-dashed line) quark model mechanism.

Table 1

Global fit parameters

	g_v	g_s	r_0(fm)	W(MeV)	V(MeV)	V_T(MeV)	V_{LS}(Mev)	r_w(fm)	a_w(fm)	χ^2	χ^2/dat
vector alone	1.1	0.0	0.85	-538	218	111	-25	0.68	0.01	2510	7.1
scalar alone	0.0	4.5	0.56	-1334	-95	38	-69	0.65	0.01	2266	6.4
vector + scalar	-17.4	6.5	0.43	-1956	147	-151	-315	0.66	0.01	1148	3.2
Kohno and Weise potential parameters			0.64	-700	-268	27	-37	0.55	0.20		

χ^2/dat is the χ^2 per data point of the fit

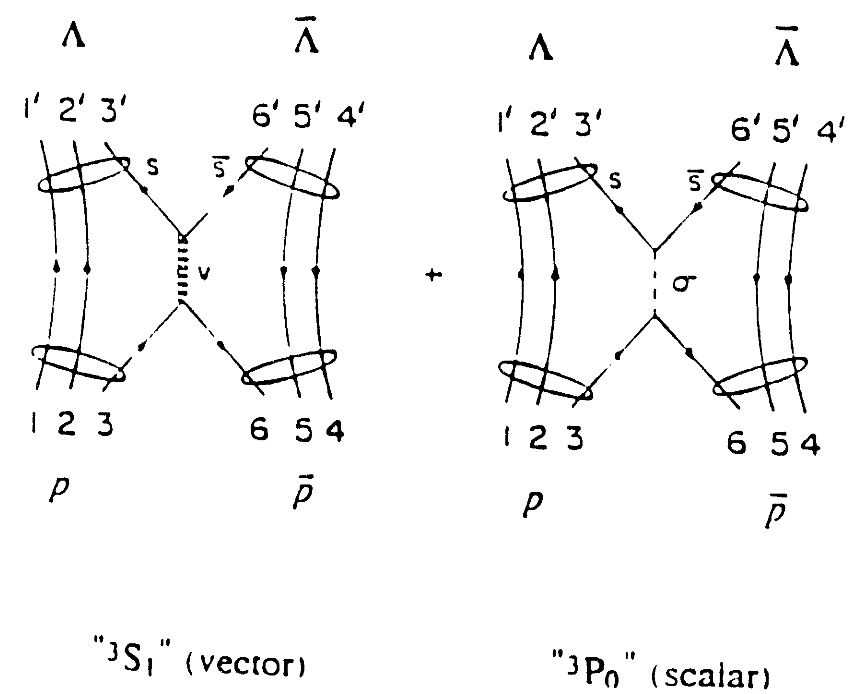
Λ
$\bar{\Lambda}$
1' 2' 3'
6' 5' 4'
s
$\bar{s}$
v
+
σ
1 2 3
6 5 4
p
$\bar{p}$
"$^3S_1$" (vector)
"$^3P_0$" (scalar)

Fig. 1

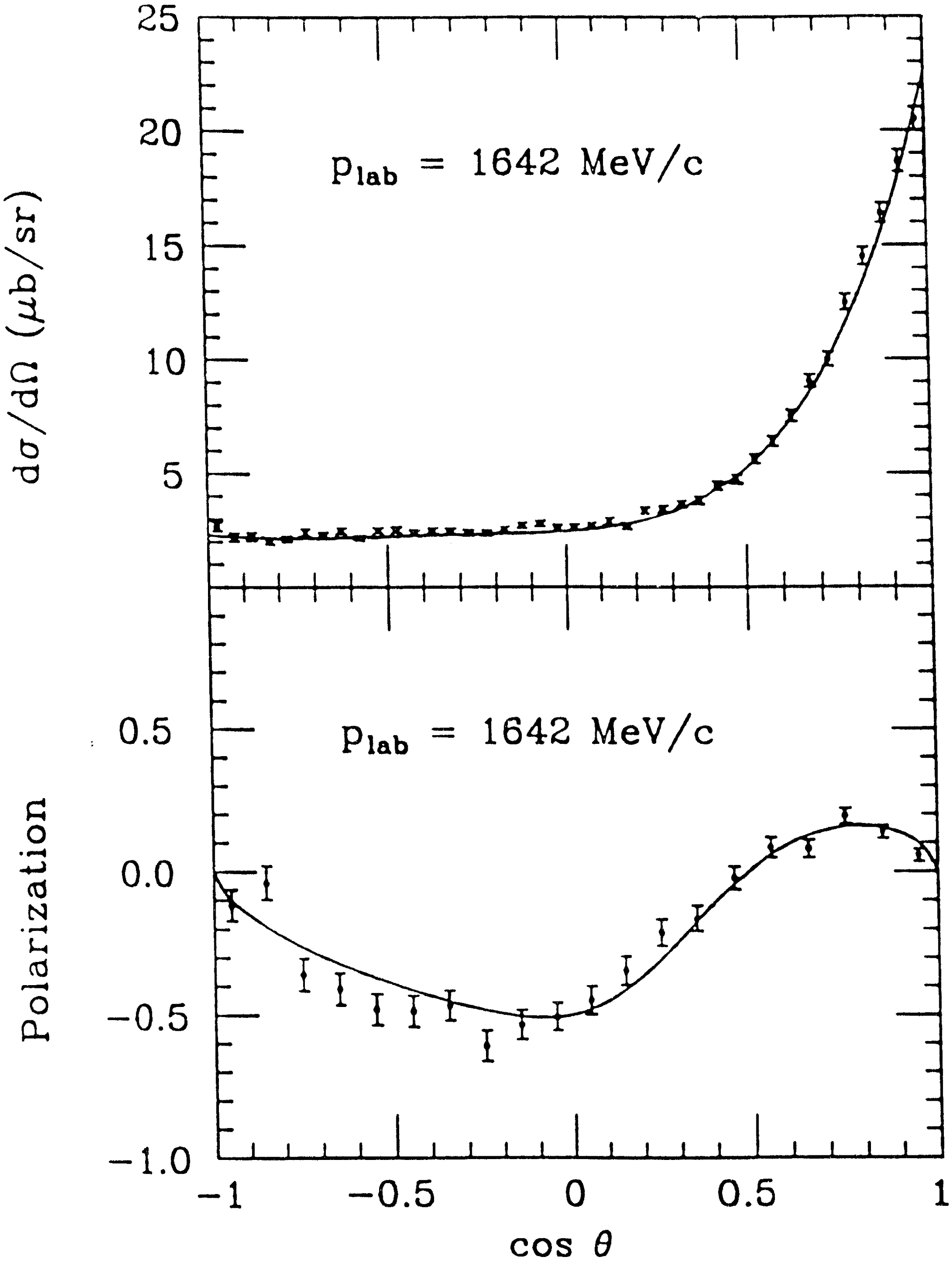

25
20
15
10
5
dσ/dΩ (μb/sr)
p_{lab} = 1642 MeV/c
0.5
0.0
−0.5
−1.0
Polarization
p_{lab} = 1642 MeV/c
−1
−0.5
0
0.5
1
cos θ

Fig. 2

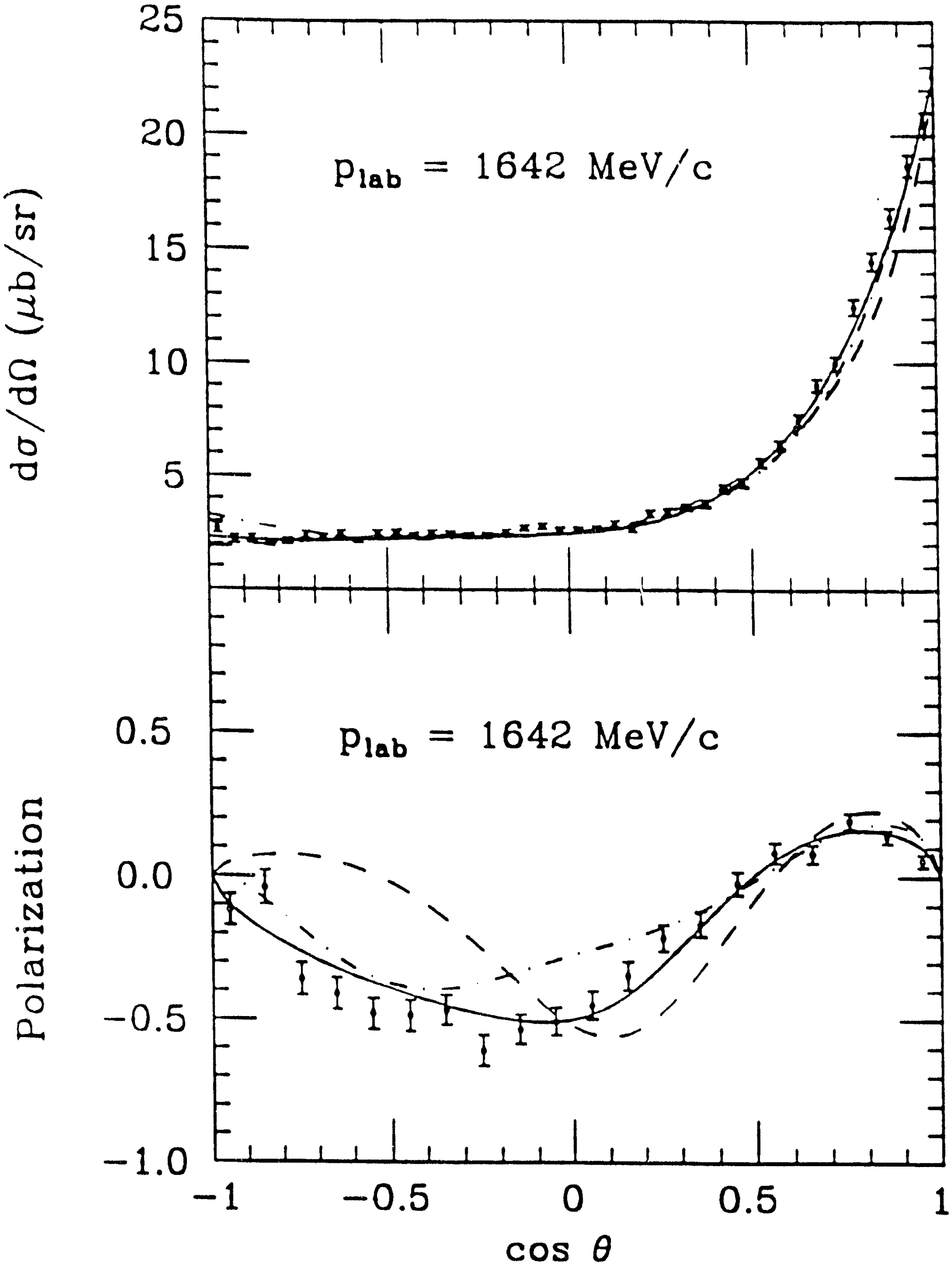

25
20
15
10
5
dσ/dΩ (μb/sr)
p_lab = 1642 MeV/c
0.5
0.0
−0.5
−1.0
Polarization
p_lab = 1642 MeV/c
−1
−0.5
0
0.5
1
cos θ

Fig. 3

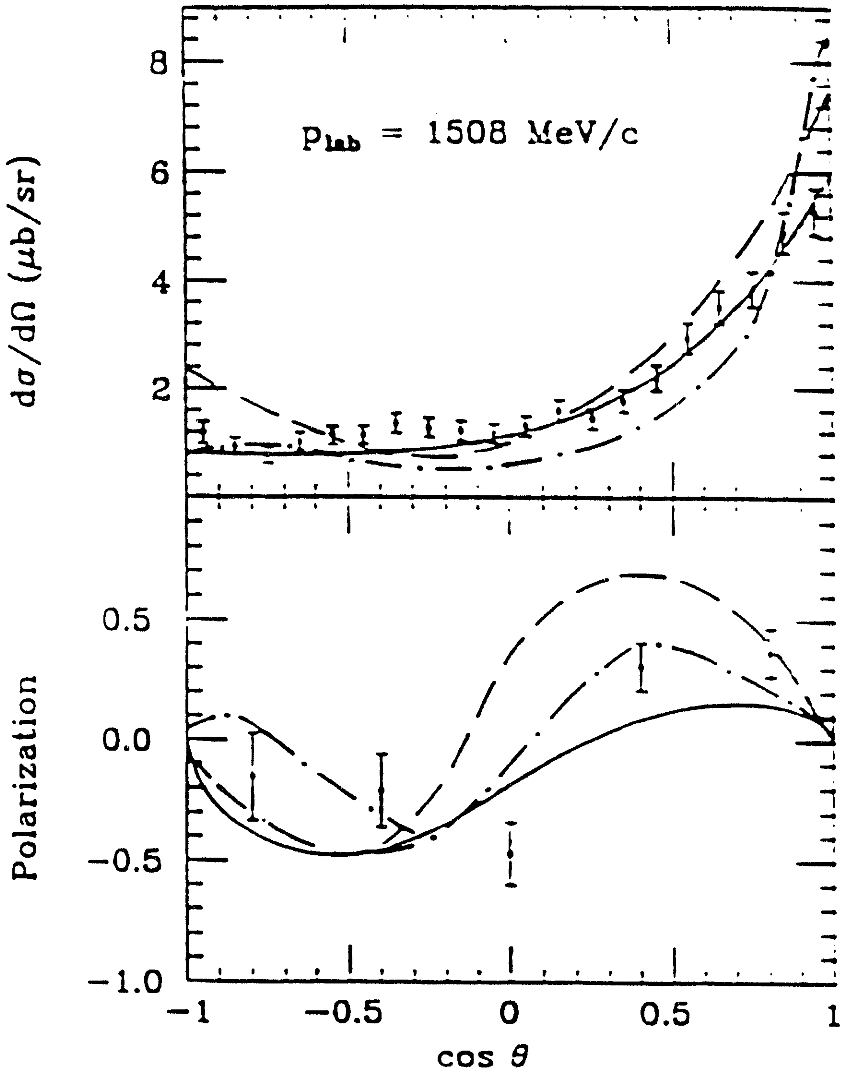

p_{lab} = 1508 MeV/c
dσ/dΩ (μb/sr)
8
6
4
2
Polarization
0.5
0.0
−0.5
−1.0
−1
−0.5
0
0.5
1
cos θ

Fig. 4

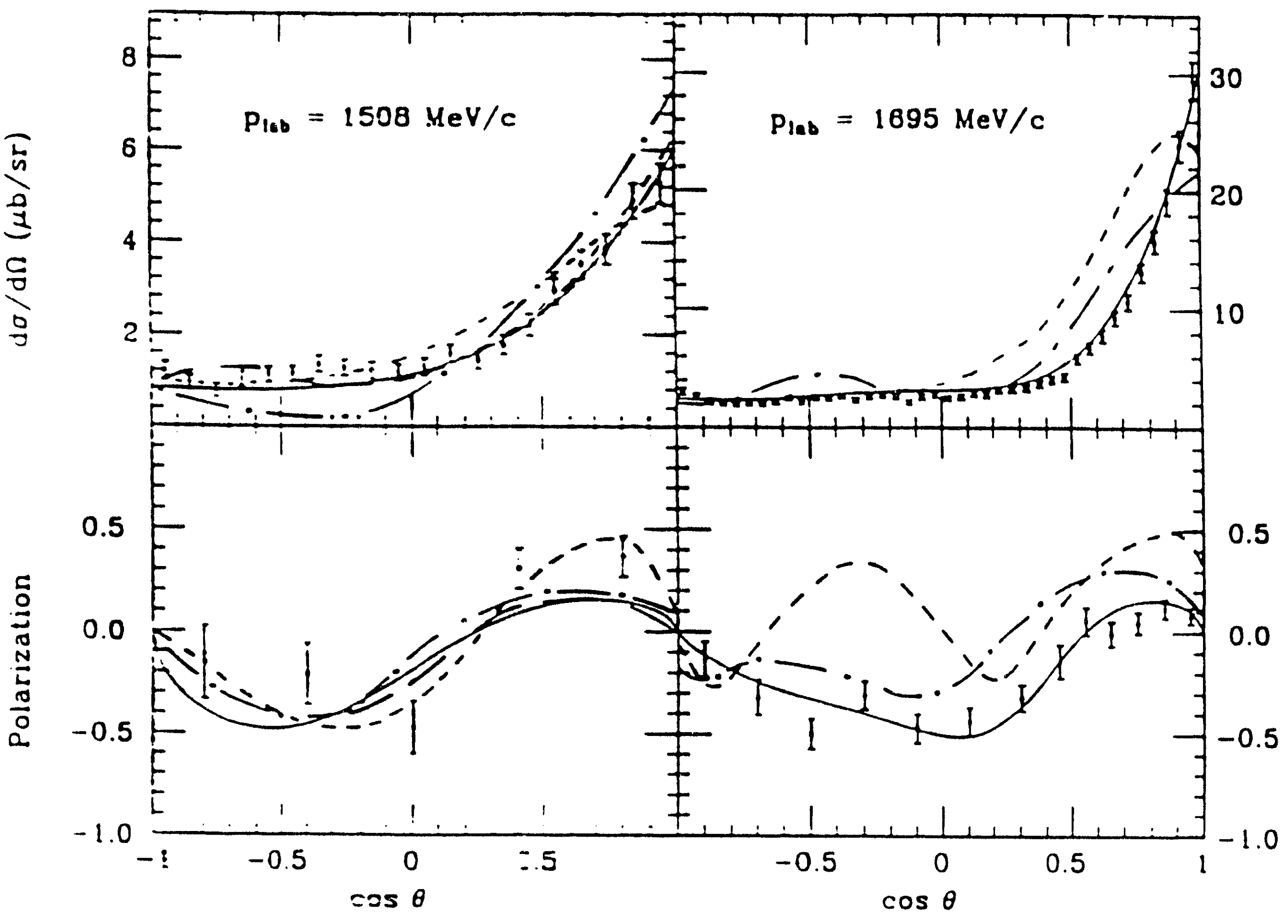

p_{lab} = 1508 MeV/c
p_{lab} = 1695 MeV/c
dσ/dΩ (μb/sr)
Polarization
cos θ
cos θ

Fig. 5

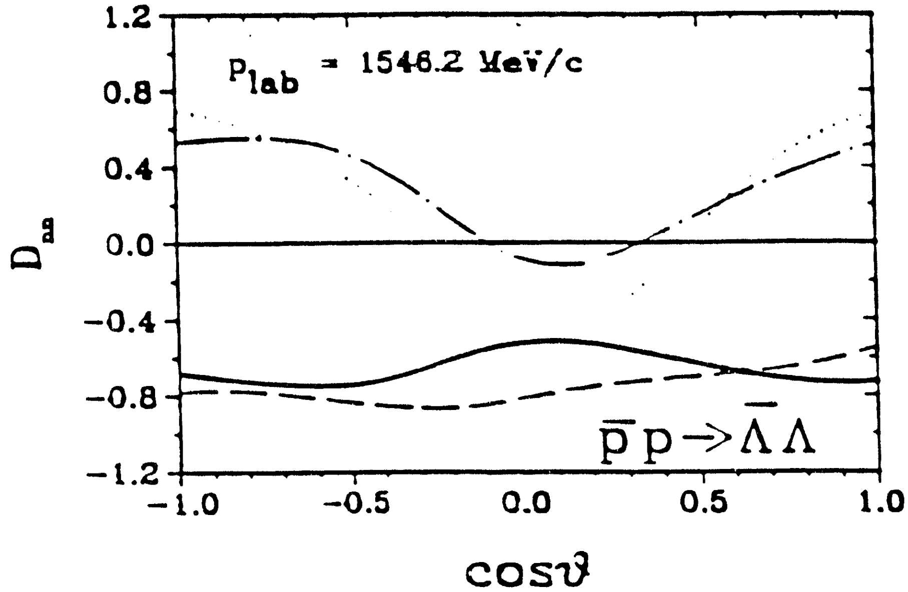
1.2
0.8
0.4
0.0
-0.4
-0.8
-1.2
D_{aa}
p_{lab} = 1546.2 MeV/c
$\bar{p}p \to \bar{\Lambda}\Lambda$
-1.0
-0.5
0.0
0.5
1.0
$\cos\vartheta$

Fig. 6

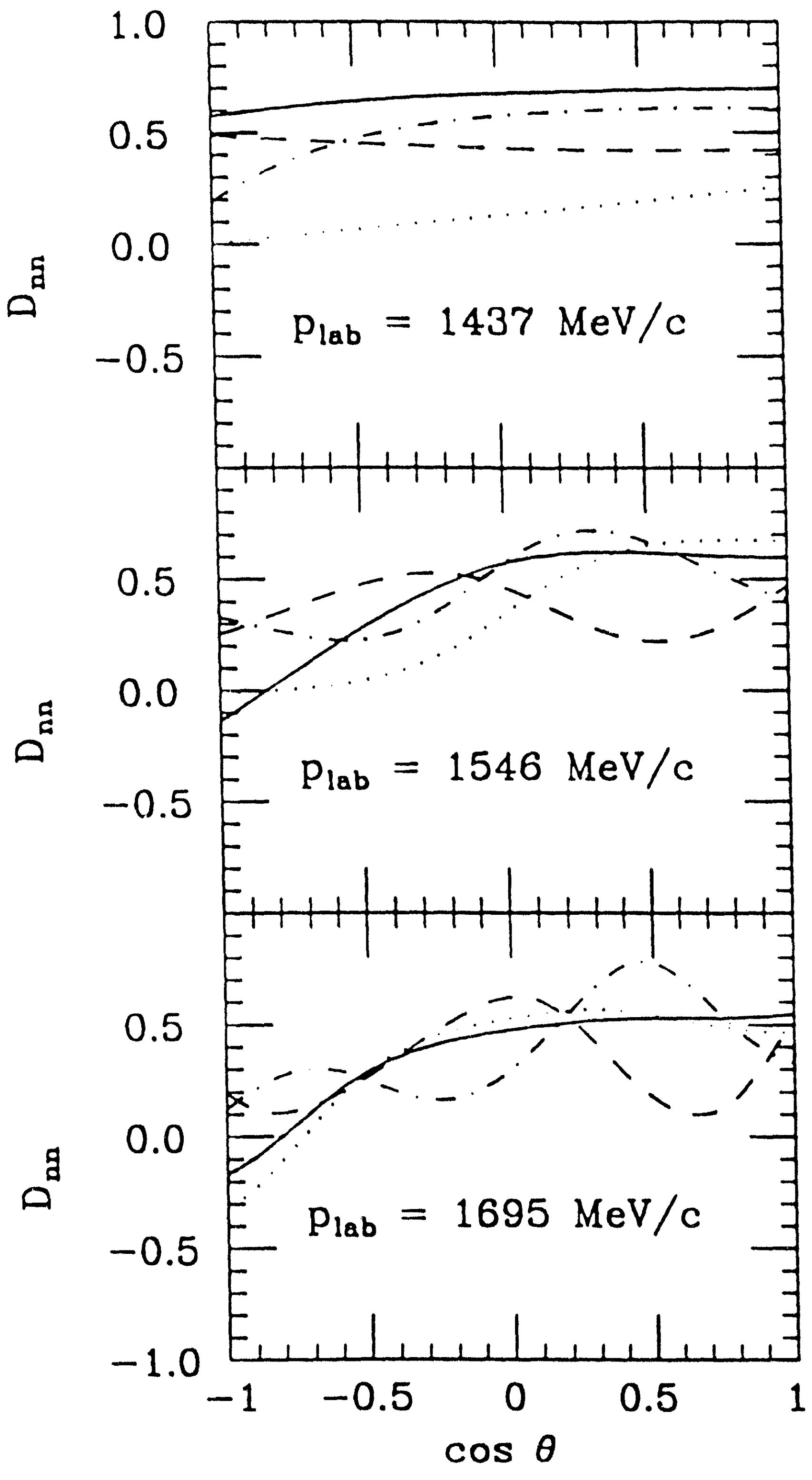
1.0
0.5
0.0
−0.5
D_{nn}
p_{lab} = 1437 MeV/c
0.5
0.0
−0.5
D_{nn}
p_{lab} = 1546 MeV/c
0.5
0.0
−0.5
−1.0
D_{nn}
p_{lab} = 1695 MeV/c
−1
−0.5
0
0.5
1
cos θ

Fig. 7

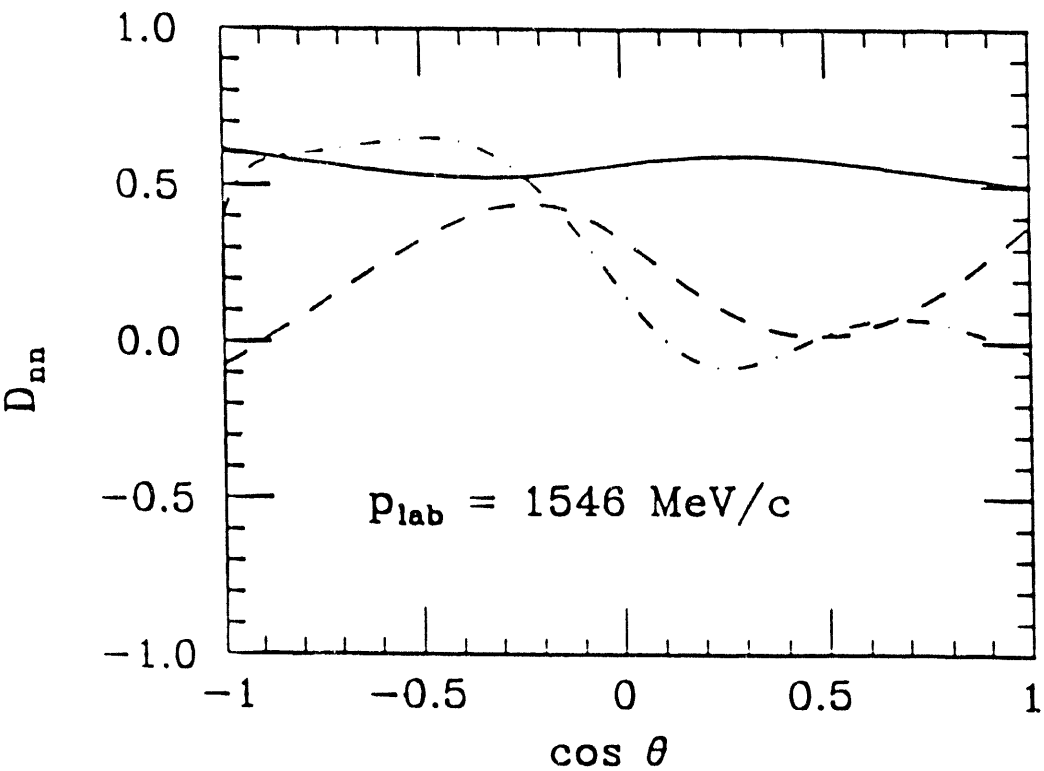

Fig. 8

DATE
FILMED
5/17/94
END